Image Vegetation Index through a Cycle Generative Adversarial Network

Patricia L. Suárez[1], Angel D. Sappa[1,2], Boris X. Vintimilla[1] and Riad I. Hammoud[3]

[1]Escuela Superior Politécnica del Litoral, ESPOL, Guayaquil, Ecuador
[2]Computer Vision Center, Campus UAB, Bellaterra, Barcelona, Spain
[3]TuSimple, 9191 Towne Centre Dr, STE 600, San Diego, CA, USA

Abstract

This paper proposes a novel approach to estimate the Normalized Difference Vegetation Index (NDVI) just from an RGB image. The NDVI values are obtained by using images from the visible spectral band together with a synthetic near infrared image obtained by a cycled GAN. The cycled GAN network is able to obtain a NIR image from a given gray scale image. It is trained by using unpaired set of gray scale and NIR images by using a U-net architecture and a multiple loss function (gray scale images are obtained from the provided RGB images). Then, the NIR image estimated with the proposed cycle generative adversarial network is used to compute the NDVI index. Experimental results are provided showing the validity of the proposed approach. Additionally, comparisons with previous approaches are also provided.

1. Introduction

Computer Vision techniques are widely used to estimate the quantity, quality and development of the vegetation. These estimations are based on the measurement of radiation's intensity of certain bands from the electromagnetic spectrum that vegetation emits or reflects. There are some solutions that use images of different spectra, therefore, sensors sensitive to each of them are needed. In the particular case of current work, which is focussed on NDVI vegetation index, registered images of the visible spectrum and infrared are needed. In other words, we need two sensors, which acquire the images at the same time from the same scene, in order to calculate the values of eq.(1). This requirement makes any solution that deals with the use of this vegetation index more expensive since it is necessary to invest in cameras sensitive to the near infrared spectrum, or a bigger platform (e.g., drone) to install all the required sensors. The current paper addresses the challenge of estimating the NDVI index by using an RGB image and a synthetically generated NIR image. In other words, it is only

necessary to have just a sensor sensitive to the visible spectrum.

A vegetation index is a single value that quantifies vegetation health or structure. The math associated with calculating a vegetation index is derived from the physics of light reflection and absorption across bands. For instance, it is known that healthy vegetation reflects light strongly in the near infrared band and less strongly in the visible portion of the spectrum. Thus, a ratio between light reflected in the near infrared and light reflected in the visible spectrum will represent areas that potentially have healthy vegetation. The more a plant absorbs visible sunlight (during the growing season), the more photosynthesis and more productive it is. Conversely, the less sunlight absorbs the plant, the less photosynthesis and less productive it is. Higher-end image processing techniques are proposed by [12], to investigate the strength of key spectral vegetation indexes for agricultural crop yield prediction using neural network in order to increase agricultural production.

Among the different indexes proposed in the literature, the Normalized Difference Vegetation Index (NDVI) is the most widely used [14]; NDVI is often used to monitor drought, forecast agricultural production, assist in forecasting fire zones and desert offensive maps. NDVI is preferable for global vegetation monitoring since it helps to compensate for changes in lighting conditions, surface slope exposure, and other external factors. In general, it is used to determine the condition, developmental stages and biomass of cultivated plants and to forecasts their yields. This index is calculated as the ratio between the difference and sum of the reflectance in NIR and red regions:

$$NVDI = \frac{R_{\mathrm{NIR}} - R_{\mathrm{RED}}}{R_{\mathrm{NIR}} + R_{\mathrm{RED}}}, \tag{1}$$

where R_{NIR} is the reflectance of NIR radiation and R_{RED} is the reflectance of visible red radiation.

According to this formula, the density of vegetation at a certain point of the image is equal to the difference in the intensities of reflected light in the red and infrared range

divided by the sum of these intensities. This index defines values from -1.0 to 1.0, basically representing greens, where negative values are mainly formed from clouds, water and snow, and values close to zero are primarily formed from rocks and bare soil. Very small values (0.1 or less) of the NDVI function correspond to empty areas of rocks, sand or snow. Moderate values (from 0.2 to 0.3) represent shrubs and meadows, while large values (from 0.6 to 0.8) indicate temperate and tropical forests.

In summary, NDVI is a measure of the health of a plant based on how the plant reflects light at certain frequencies (some waves are absorbed and others are reflected). Chlorophyll (a health indicator) strongly absorbs visible light, and the cellular structure of the leaves strongly reflect near-infrared light. When the plant becomes dehydrated, sick, affected with disease, etc., the spongy layer deteriorates, and the plant absorbs more of the near-infrared light, rather than reflecting it. Thus, observing how NIR changes compared to red light provides an accurate indication of the presence of chlorophyll, which correlates with plant health. Recent studies have demonstrated the usefulness of optical indexes from hyperspectral or cross-spectral remote sensing in the assessment of vegetation biophysical variables both in forestry and agriculture [22], [1]. Those indexes are, however, the combined response to variations of several vegetation and environmental properties, such as Leaf Area Index (LAI), leaf chlorophyll content, canopy shadows, and background soil reflectance [7].

Cross/multi-spectral computer vision approaches provide unique solutions to multiple complex problems, however, as mentioned above, different preprocessing steps need to be implemented before computing these solutions; hence, in the current work we present a novel approach to obtain a NDVI image, but just using information from a single spectral band. Actually, a similar technique has been recently presented in [17] where vegetation index is estimated based on a learning model using only a single near infrared spectral band image. Although interesting results have been obtained, the weakness point of that approach lies on the need of having NIR images, which are not that much common like visible spectrum images. In the current work we propose to explore the possibility to estimate NDVI vegetation index using images from the visible spectrum. The index is estimated from a learning based approach, where a Cycle Generative Adversarial Network (CycleGAN) is trained with a large data set. Additionally, a more elaborated loss function is proposed to preserve details of the estimated NIR images, which are used later on to obtain the vegetation index NDVI. In our approach, a set of unpaired images are used as input, one for visible spectrum and the other from the NIR spectrum, each one is fed into a CycleGAN to obtain a synthetic NIR image, using a multiple loss function, a residual network (RESNET) architecture is used

to go deeper without degradation in accuracy and error rate. The manuscript is organized as follows. Section 2 presents works related to the NDVI index problems, as well as the basic concepts and notation of GAN and CycleGAN networks. The proposed approach is detailed in section 3. The experimental results with a set of real images are presented in section 4. Finally, the conclusions are given in section 5.

2. Related Work

Solutions based on computer vision to tackle problems related to precision agriculture have been widely used. This technology enables better identification, analysis, and management of this temporal and spatial in-field variability. The aforementioned precision, is all about reducing this variability through more focused and targeted efforts which should increase production by maintaining crop quality and quantity [13]. Remote sensing in precision agriculture makes use of sensors and vegetation indexes [15]. Normally, vegetation index is calculated using different spectral bands, usually depending on what type of information is trying to be obtained. In this particular case of this work the NDVI vegetation index is estimated. Lately, in this field of study, many traditional techniques or convolutional neural networks based solutions have been proposed.

In [4], Filippa et al. has proposed a time series of vegetation indexes (e.g., normalized difference vegetation index [NDVI]) and color indexes (e.g., green chromatic coordinate [GCC]) based on radiometric measurements by means of near-surface remote sensing (e.g., spectral sensors or digital cameras) to describe ecosystem phenology. Zheng et al. [23] propose a method using a stepwise cluster analysis (SCA), to address and represent the complex and nonlinear relations between climatic factors and NDVI. Accordingly, the knowledge of vegetation dynamics in response to climate change would need to be further reflected and expanded. In [20], Testa et al. has proposed a technique to monitoring forest phenology, which allows to study the effects of climate change on vegetated land surfaces, in order to find the best VI/TS combination to estimate start-of-season (SOS) and end-of-season (EOS) dates across 50 temperate deciduous forests. In [5] the author has proposed the use of the MODIS sensors that appears to be appropriate for identifying landscape patterns, time series, change detection maps, and the potential impacts from climate change for each area of study. These patterns of vegetation types can be inventoried at a 250m resolution and monitored at a high temporal resolution. In [21] the authors have proposed a method to predict the habitat quality of protected dry grasslands using Landsat NDVI phenology, in order to infer a representation of local productivity and management pattern.

Recently, Generative Adversarial Network based learning techniques have been used obtaining appealing results;
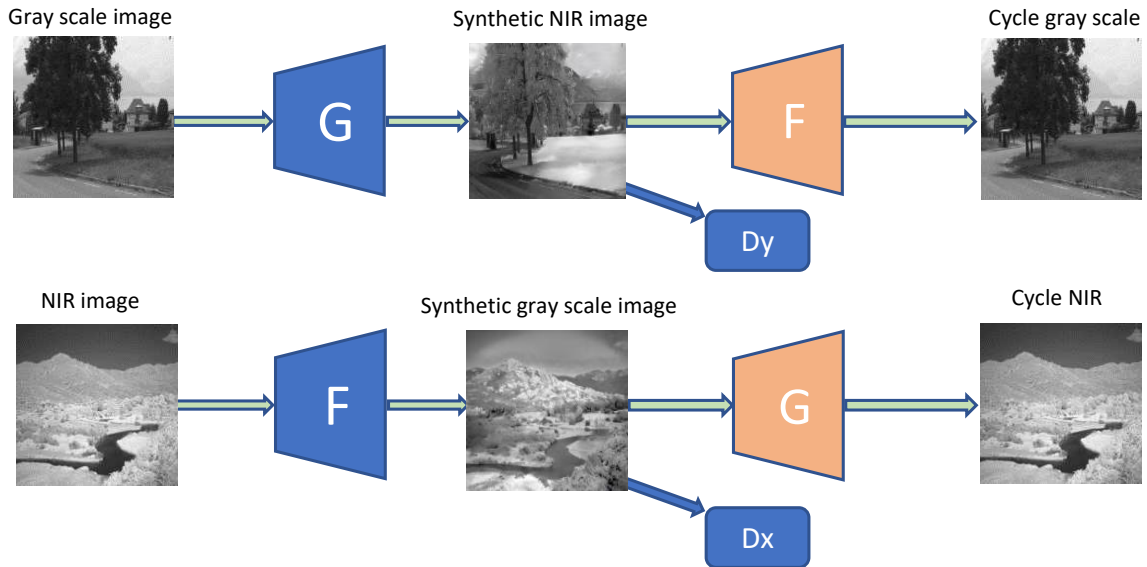
Figure 1. Cycle Generative Adversarial model implemented on the current work to estimate the NIR representation.

actually, in most of the cases they are among the best options, (e.g., see [2]). These (GAN) networks are becoming the dominant tool to tackle most of computer vision problems. GANs are powerful and flexible tools, one of their most common application is image generation. In the GAN framework [6], generative models are estimated via an adversarial process, in which simultaneously two models are trained: i) a generative model G that captures the data distribution, and ii) a discriminative model D that estimates the probability that a sample came from the training data rather than G. The training procedure for G is to maximize the probability of D making a mistake. In this architecture it is possible to apply certain conditions to improve the learning process. According to [11], to learn the generators distribution p_g over data x, the generator builds a mapping function from a prior noise distribution $p_z(z)$ to a data space $G(z; \theta_g)$. The discriminator, $D(x; \theta_d)$, outputs a single scalar representing the probability that x came from training data rather than p_g. G and D are both trained simultaneously, the parameters for G are adjusted to minimize $log(1 - D(G(z)))$ and for D to minimize $logD(x)$. Some works are presented on [16], [18] for image colorization or [19] for vegetation index estimation. In [9] Isola et al. have proposed a conditional adversarial network as a general-purpose solution to image-to-image translation problems. This network not only learns the mapping from input image to output image, but also learns a loss function to train this mapping. This makes it possible to apply the same generic approach to problems that traditionally would require very different loss formulations. Then, new approaches are presented that allow learning to translate be-

tween domains without examples of paired input-output. In [24] the authors present a system that can learn to capture special characteristics of one image collection and figuring out how these characteristics could be translated into the other image collection, all in the absence of any paired training examples, converting an image from one representation of a given scene, x, to another, y, e.g., grayscale to color, image to semantic labels, edge-map to photograph.

3. Proposed Approach

This section presents the approach proposed for NDVI index vegetation estimation just with a single image from the visible spectrum. As mentioned above, it uses a similar architecture like the one proposed on [24], a recent work for unpaired image to image translation, where the usage of a cycle generative adversarial network (CycleGAN) has been proposed. CycleGANs is a convenient method for image-to-image translation problems, such as style transfer, because it just rely on an unconstrained input set and output set rather than specific corresponding input/output pairs. This could be time-consuming, unfeasible, or even impossible based on what two image types are being trying to translate between. Another approach presented in [9] has shown results synthesizing photos from label maps, reconstructing objects from edge maps, but still dependent on some kind of correlated labeling.

Our architecture is based on the approach presented in [24] in relation to cycle consistent learning and loss functions; in our work it is used to estimate the synthetic NIR images. The proposed model can learn to translate the im-

ages between the visible spectrum to their corresponding NIR spectrum, without the need to have accurately registered RGB/NIR pairs. This allows us to use these NIR synthetic images in the calculation of the NDVI vegetation index and to be able to use them in solutions oriented to solve problems related to the state of the crops and their corresponding level of productivity in the crops. Another advantage of being able to count on the synthetic images of the NIR spectrum is that, undoubtedly, the costs of the solutions are decreased since there is no need to buy acquisition devices sensitive to that electromagnetic spectrum. Additionally, our architecture uses Residual Network (ResNET) [8] to perform the image transformation from one spectrum to another. It avoids the vanishing gradient problem, as the gradient is back-propagated to earlier layers, repeated multiplication may make the gradient infinitely small. As a result, as the network goes deeper, its performance can get saturated or even starts degrading rapidly. To avoid all this problems, we implement our generator and discriminator to propagate larger gradients to initial layers and these layers also could learn as fast as the final layers, giving us the ability to train deeper networks. Resnet is a model designed to be applied in a deep neural network layer architecture, which consists of convolution layers known as building block, where a residue of input is added to the output.

The core idea of ResNet is to introduce a so-called identity shortcut connection that skips one or more layers. These skip connections ensure properties of NIR images of previous layers are available for later layers as well, so that their output do not deviate much from original RGB input, otherwise the characteristics of original images will not be retained in the output and results will be very unreal. Figure 1 depicts the CycleGAN model proposed in the current work. As can be appreciated in Figure 1, CycleGan architecture to generate NIR synthetic images is composed of two generators G, F and two discriminators Dx, Dy. In order to generate a synthetic image, the architecture takes the advantage from the joint of cycle-consistency and least square losses [10] in addition to the usual discriminator and generator losses. The results of the experiments have shown that these loss functions demand that the model maintain textural information of the visible and NIR images and generate uniform synthetic outputs. According with [24] the objective of a CycleGAN is to learn mapping functions between two domains X and Y given training samples $x_{i_{i=1}}^{N} \in X$ and $x_{i_{i=1}}^{N} \in Y$.

The model includes two mappings functions $G : X \rightarrow Y$ and $F : Y \rightarrow X$. In addition, it introduces two adversarial discriminators D_x and D_y, where D_x aims to distinguish between images x and translated images $F(y)$; in the same way, D_y aims to discriminate between y and $G(x)$. Besides, the proposed approach includes two types of loss terms: adversarial losses [6] for matching the distribution

of generated synthetic NIR images to the data distribution in the target domain real NIR images; and a cycle consistency loss to prevent the learned mappings G and F from contradicting each other. The adversarial losses according to [6] to both mapping functions. For the mapping function $G : X \rightarrow Y$ its discriminator D_y, is defined as:

$$\mathcal{L}_{GAN}(G, D_y, X, Y) = \mathbb{E}_{y \sim p\ \text{data}_{(y)}}[log D_Y(y)] + \quad (2)$$
$$\mathbb{E}_{x} \sim_{p\ \text{data}_{(x)}}[log(1 - D_Y(G(x)))],$$

where G tries to generate images $G(x)$ that look similar to images from domain Y, while D_y aims to distinguish between translated samples $G(x)$ and real samples y.

For the mapping function $F : Y \rightarrow X$ its discriminator D_x, is defined as:

$$\mathcal{L}_{GAN}(F, D_x, Y, X) = \mathbb{E}_{x \sim p\ \text{data}_{(x)}}[log D_X(x)] + \quad (3)$$
$$\mathbb{E}_{y} \sim_{p\ \text{data}_{(y)}}[log(1 - D_X(G(y)))],$$

where F tries to generate images $F(y)$ that look similar to images from domain X, while D_x aims to distinguish between translated samples $F(y)$ and real samples x.

Also, according to [24], to reduce the space of possible mapping functions, they argue that the learned mapping functions should be cycle-consistent, for each image x from domain X, the image translation cycle should be able to bring x back to the original image, i.e., $x \rightarrow F(G(x)) \rightarrow G(x) \approx x$, calling this forward cycle consistency. Therefore, for each image y from domain Y, G and F should also satisfy backward cycle consistency: $y \rightarrow F(y) \rightarrow G(F(y)) \approx y$. This cycle consistency loss is defined as :

$$\mathcal{L}_{cycle}(G, F) = \mathbb{E}_{x \sim p\ \text{data}_{(x)}}[\|F(G(x)) - x\|_1] + \quad (4)$$
$$\mathbb{E}_{y} \sim_{p\ \text{data}_{(y)}}[\|G(F(y)) - y\|_1].$$

A least square loss has been implemented [10] to accelerate the training process. This loss is able to move the fake samples toward the decision boundary, in other words, generate samples that are closer to real data, in our case the synthetic NIR image. The experiments performed with this loss instead of negative log likelihood shown better results. The equations (2) and (3) are replaced with the least square losses, which are defined as :

$$\mathcal{L}_{LSGAN}(G, D_y, X, Y) = \mathbb{E}_{y \sim p\ \text{data}_{(y)}}[(D_Y(y) - 1)^2] + \quad (5)$$
$$\mathbb{E}_{x} \sim_{p\ \text{data}_{(x)}}[D_Y(G(x))^2],$$

Once the NIR image is estimated the NDVI index is computed by using eq. (1) together with the information from the red channel of the given image.

Figure 2. Illustration of NIR images obtained by the proposed CycleGAN, which are later on used to estimate the corresponding NDVI indexes. ($1st.row$) RGB images. ($2nd.row$) Gray scale image used as input into the CycleGAN. ($3rd.row$) Estimated NIR images. ($4th.row$) Ground truth NIR images. Images from [3], *country*, *field* and *mountain* categories.

4. Experimental Results

The proposed approach, see Fig. 1, has been evaluated using NIR and RGB images obtained from eq. (1), in which the RGB red channel was used; the cross-spectral data set used in our implementation came from [3]. This dataset consists of 477 registered images categorized into 9 groups captured in RGB (visible) and NIR (Near Infrared) spectral bands. The *country*, *mountain* and *field* categories have

been considered for evaluating the performance of the proposed approach, examples of this dataset are presented in Fig. 2. The *country* category contains 52 pairs of images of (1024×680 pixels), *mountain* category contains 55 pairs of images of (1024×680 pixels), while the *field* contains 51 pairs of images of (1024×680 pixels). In order to increase the training dataset a data augmentation process was performed, to improve the accuracy of our network to generate
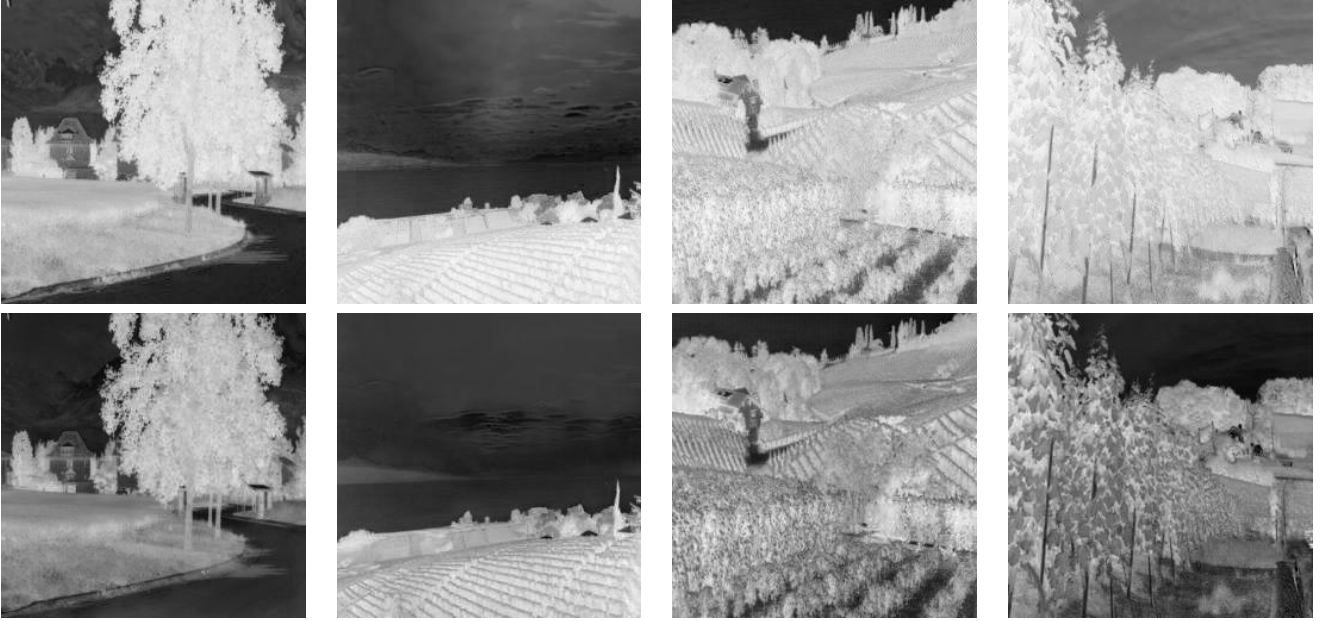
Figure 3. Images of NDVI vegetation indexes obtained with the synthetic NIR generated by the proposed CycleGAN. (*top*) Ground truth NDVI vegetation index images. (*bottom*) Estimated NDVI vegetation indexes. Images from [3], *country*, *field* and *mountain* categories.

synthetic NIR images. The data augmentation consists of applying flipping, rotating and transposing over the original images. After the data augmentation process, for each category 600 pairs of images from visible and NIR spectrum have been generated. Additionally, for each category 40 pairs of images for testing and 20 pairs of images for validation from visible and NIR spectrum have been used. It is important to emphasize that despite the images are registered, for the CycleGAN training process of our model, which estimates the synthetic NIR image, we use unpaired images.

On average, every training process took about 80 hours using a 3.2 GHz eight core processor with 32GB of memory with a NVIDIA TITAN XP GPU. Some illustrations, with the corresponding NIR results obtained with the proposed CycleGAN approach are depicted in Fig. 2 for qualitative evaluation.

Results from the Cycle Generative Adversarial network (synthetic NIR images) are then used for estimating the NDVI indexes. Figure 3 presents some illustrations of NDVI indexes estimated from these NIR images and the ground truth ones computed from eq. (1). Quantitative evaluations are presented in Table 1. In this table average root mean square error (RMSE) and structural similarity index metric (SSIM) computed over the validation set are depicted, when different combinations of the proposed loss functions where considered. Our experiments used the standard loss function for GANs, which are based on negative log likelihood and also used the least square

loss, which obtain better quantitative results and avoid the vanishing gradient problem, where a deep feed-forward network is unable to propagate valid gradient information from the output back to the first layer of the model. We implement least square loss to accelerate and maintain stable the training process. Additionally, in this table, results from [19] are presented. It can be appreciated that in all the cases the results obtained with the least square loss in the proposed CycleGAN are better than those obtained with the approach presented in [19]. It should be mentioned that the least square losses permits to accelerate the network convergence, allowing a better optimization of the network.

To increase the cyclic loss effect over the network we used $L1\ (\lambda)$. The CycleGAN network proposed has been trained using Stochastic AdamOptimazer since it is well suited for problems with deep network, large datasets and avoid overfitting. The image dataset was normalized in a (-1,1) range and rescaled to 256x256 to avoid memory problems during the training process. The following hyperparameters were used during the training process: learning rate 0.0003; epsilon = 1e-08; exponential decay rate for the 1st moment momentum 0.6; $L1\ (\lambda)$ 10.5; weight decay 1e-2; leak relu 0.20.

5. Conclusions

This paper tackles the challenging problem of generating NDVI vegetation index using a NIR synthetic image and their corresponding RGB representation. NIR images

Table 1. Average Root Mean Squared Errors (RMSE) and Structural Similarities (SSIM) obtained from the estimated NDVI vegetation index and the real one computed from eq. (1) (SSIM the bigger the better). Note NDVI values are scaled up to a range of [0-255] since they are depicted as images as shown in Fig. 3

Training	RMSE			SSIM		
	country	*field*	*mountain*	*country*	*field*	*mountain*
Results from [19]	3.53	3.70	–	0.94	0.91	–
NDVI estimation with synthectic NIR $\mathcal{L}_{CycleGan}$	3.42	3.64	3.63	0.94	0.91	0.86
NDVI estimation with synthectic NIR $\mathcal{L}_{CycleGan} + \mathcal{L}_{LsGan}$	3.39	3.56	3.81	0.94	0.92	0.89

are estimated by using a CycleGan network. Results have shown that in most of the cases the network is able to obtain reliable synthetic NIR representations that can be used to obtain vegetation indexes. As mentioned in the discussion section, this approach has not the limitation of needing paired NIR-RGB images for training. As a future work, actually, as work in progress we are considering the usage of a CycleGAN architecture with continual learning with deep generative display, but feed it with RGB and their corresponding NIR image in the generator to speed up the generalization. Future work will also consider other loss functions to improve the training process.

Acknowledgment

References

[1] T. Adão, J. Hruška, L. Pádua, J. Bessa, E. Peres, R. Morais, and J. Sousa. Hyperspectral imaging: A review on uav-based sensors, data processing and applications for agriculture and forestry. *Remote Sensing*, 9(11):1110, 2017. 2

[2] M. Arjovsky and L. Bottou. Towards principled methods for training generative adversarial networks. *arXiv preprint arXiv:1701.04862*, 2017. 3

[3] M. Brown and S. Süsstrunk. Multi-spectral SIFT for scene category recognition. In *Computer Vision and Pattern Recognition (CVPR), 2011 IEEE Conference on*, pages 177–184. IEEE, 2011. 5, 6

[4] G. Filippa, E. Cremonese, M. Migliavacca, M. Galvagno, O. Sonnentag, E. Humphreys, K. Hufkens, Y. Ryu, J. Verfaillie, U. M. di Cella, et al. Ndvi derived from near-infrared-enabled digital cameras: Applicability across different plant functional types. *Agricultural and Forest Meteorology*, 249:275–285, 2018. 2

[5] T. W. Gillespie, S. Ostermann-Kelm, C. Dong, K. S. Willis, G. S. Okin, and G. M. MacDonald. Monitoring changes of ndvi in protected areas of southern california. *Ecological Indicators*, 88:485–494, 2018. 2

[6] I. Goodfellow, J. Pouget-Abadie, M. Mirza, B. Xu, D. Warde-Farley, S. Ozair, A. Courville, and Y. Bengio. Generative adversarial nets. In *Advances in neural information processing systems*, pages 2672–2680, 2014. 3, 4

[7] D. Haboudane, J. R. Miller, N. Tremblay, P. J. Zarco-Tejada, and L. Dextraze. Integrated narrow-band vegetation indices for prediction of crop chlorophyll content for application to precision agriculture. *Remote sensing of environment*, 81(2-3):416–426, 2002. 2

[8] K. He, X. Zhang, S. Ren, and J. Sun. Deep residual learning for image recognition. In *Proceedings of the IEEE conference on computer vision and pattern recognition*, pages 770–778, 2016. 4

[9] P. Isola, J.-Y. Zhu, T. Zhou, and A. A. Efros. Image-to-image translation with conditional adversarial networks. In *Proceedings of the IEEE conference on computer vision and pattern recognition*, pages 1125–1134, 2017. 3

[10] X. Mao, Q. Li, H. Xie, R. Y. Lau, Z. Wang, and S. Paul Smolley. Least squares generative adversarial networks. In *Proceedings of the IEEE International Conference on Computer Vision*, pages 2794–2802, 2017. 4

[11] M. Mirza and S. Osindero. Conditional generative adversarial nets. *arXiv preprint arXiv:1411.1784*, 2014. 3

[12] S. S. Panda, D. P. Ames, and S. Panigrahi. Application of vegetation indices for agricultural crop yield prediction using neural network techniques. *Remote Sensing*, 2(3):673–696, 2010. 1

[13] D. I. Patrício and R. Rieder. Computer vision and artificial intelligence in precision agriculture for grain crops: a systematic review. *Computers and Electronics in Agriculture*, 153:69–81, 2018. 2

[14] J. Rouse Jr, R. Haas, J. Schell, and D. Deering. Monitoring vegetation systems in the great plains with erts. 1974. 1

[15] V. Sitokonstantinou, I. Papoutsis, C. Kontoes, A. Lafarga Arnal, A. Armesto Andrés, and J. Garraza Zurbano. Scalable parcel-based crop identification scheme using sentinel-2 data time-series for the monitoring of the common agricultural policy. *Remote Sensing*, 10(6):911, 2018. 2

[16] P. L. Suarez, A. D. Sappa, and B. X. Vintimilla. Colorizing infrared images through a triplet conditional dcgan architecture. In *19th International Conference on Imaage Analysis and processing*, 2017. 3

[17] P. L. Suárez, A. D. Sappa, and B. X. Vintimilla. Learning image vegetation index through a conditional generative adversarial network. In *2nd Ecuador Technical Chapters Meeting*, 2017. 2

[18] P. L. Suarez, A. D. Sappa, and B. X. Vintimilla. Learning to colorize infrared images. In *15th International Conference on Practical Applications of Agents and Multi-Agent Systems*, 2017. 3

[19] P. L. Suárez, A. D. Sappa, and B. X. Vintimilla. Vegetation index estimation from monospectral images. In *International Conference Image Analysis and Recognition*, pages 353–362. Springer, 2018. 3, 6, 7

[20] S. Testa, K. Soudani, L. Boschetti, and E. B. Mondino. Modis-derived evi, ndvi and wdrvi time series to estimate phenological metrics in french deciduous forests. *International journal of applied earth observation and geoinformation*, 64:132–144, 2018. 2

[21] D. Weber, G. Schaepman-Strub, and K. Ecker. Predicting habitat quality of protected dry grasslands using landsat ndvi phenology. *Ecological Indicators*, 91:447–460, 2018. 2

[22] M. Wójtowicz, A. Wójtowicz, and J. Piekarczyk. Application of remote sensing methods in agriculture. *Communications in Biometry and Crop Science*, 11(1):31–50, 2016. 2

[23] Y. Zheng, J. Han, Y. Huang, S. R. Fassnacht, S. Xie, E. Lv, and M. Chen. Vegetation response to climate conditions based on ndvi simulations using stepwise cluster analysis for the three-river headwaters region of china. *Ecological indicators*, 92:18–29, 2018. 2

[24] J.-Y. Zhu, T. Park, P. Isola, and A. A. Efros. Unpaired image-to-image translation using cycle-consistent adversarial networks. In *Proceedings of the IEEE International Conference on Computer Vision*, pages 2223–2232, 2017. 3, 4